Synthesis of Hybrid Nanocapsules by Miniemulsion (Co)polymerization of Styrene and γ-Methacryloxypropyltrimethoxysilane

Ke-Fan Ni, Guo-Rong Shan,* and Zhi-Xue Weng

State Key Laboratory of Chemical Engineering, Polymer Reaction Engineering Division, Department of Chemical and Biochemical Engineering, Zhejiang University, Hangzhou 310027, China

Received September 22, 2005; Revised Manuscript Received January 12, 2006

ABSTRACT: Hybrid nonacapsules are synthesized by miniemulsion (co)polymerization of styrene and 3-trimethoxysilylpropylmethacrylate silane (MPS) in one step. Hydrocarbon droplets are encapsulated by organic−inorganic hybrid material, which is formed by simultaneous free radical polymerization reaction and hydrolysis−condensation reaction of organosilane in MPS. The morphology and the microstructure are characterized by transmission electron microscopy (TEM), dynamic light scattering (DLS), solid-state NMR, and infrared (IR) spectroscopy. The capsule morphology is achieved by polymerization inducing phase separation within minidroplets dispersed in aqueous phase. The feasibility of the final morphology is analyzed by thermodynamic and kinetic factors first. Particle nucleation processes with different formulation are followed by DLS, and it has a great influence on the latex morphology. Monomer/hydrocarbon ratio in the droplets and MPS fraction in the capsules are also of great important to the morphology due to their influence on phase separation behavior and mechanic properties of capsules, respectively. Finally, the loading and releasing processes of this capsule are monitored by ultraviolet−visible (UV) measurement.

Introduction

The control of the morphology of latex particles has been an intensive area in colloidal polymer science. Technology has advanced such that a variety of structured particles are nowadays accessible including core−shell, microdomain, and interpenetrating network latexes. These advances have been based on a deepening understanding of the thermodynamic and kinetic aspect of synthetic process, especially emulsion polymerization process, as well as more sophisticated approaches to processing. Synthetic methods leading to particles having voids have also been extensively investigated. Here, we are interested in the special case of a hollow sphere or nanocapsule structure.

Hollow latex is characterized with outer shell and inner void cavity. The outer shell may be organic, inorganic, or hybrid materials, while the cavity inside the hollow sphere can be filled with a kind of liquids. Thus, it can be applied in a variety of domains ranging from the high quality coating because of its special optic and mechanical properties to the controlled release of active substances. Up to now, predominantly the formation of capsules with a size of 1 μm and larger is described. However, for many applications, especially in medicine and high-resolution electronic inks, smaller capsules between 50 and 300 nm are of high interest.

A variety of hollow capsules in this scale have been synthesized via different strategies in recent years. Templating approaches have extensively developed as means to mold the shape and control the size of the capsules. This approach requires in a previous step the use of nanocoating technologies to elaborate core−shell material with uniform and surface characteristics. The coating technologies include seeded growth technique adapted from the Stöber method,[1,2] in-situ polymerization on the surface of template,[3,4] and layer-by-layer self-assembly through electrostatic attraction.[5−7]

Direct emulsion polymerization technology is another highly studied approach to elaborate nanocapsule aside from the above strategy. One prominent technique involves making a structured particle with a carboxylated core polymer and outer shell. Ionization of the core material with bases under convenient conditions expands the core by "osmotic swelling" and produces hollow spheres containing water and polyelectrolyte in the interior.[8] A second developed approach involves a dispersed ternary system composed of monomer, oil, and water. The oil phase is a nonsolvent for the polymer being formed, and phase separation is taking place during the polymerization process to form capsule with hydrocarbon inside.[9] Landfester et al. described a similar approach preparing polymeric nanocapsules by miniemulsion polymerization.[10]

The incorporation of functional groups into polymer latexes is another major interest in the field of colloidal polymer science. Among this interest, functionalization of inorganic oxides (mainly silica) into polymer is highly researched because it leads to organic−inorganic hybrid structures, which have a lot of potential applications in various industry domains. It can be easily realized by the reaction of silanol groups with alcohols, organoalkoxysilanes, and chorolsilanes,[11] and the copolymerization approach (direct polymerization of suitable functional comonomers) is believed particularly well suited to control the hybrid structures and surface properties.[12] Therefore, it must be of great interest if inorganic silica is incorporated into the outer shell of nanocapsules through direct heterophase copolymerization such as emulsion or miniemulsion polymerization processes.

In this paper, since nanocapsules can be synthesized by miniemulsion polymerization in one step and functional silane groups can be conveniently incorporated by copolymerization approach, a miniemulsion polymerization is developed that yields an encapsulation of a nonsolvent hydrocarbon by (co)-polymer being formed. Inorganic silica is incorporated by copolymerization using 3-trimethoxysilylpropyl methacrylate (MPS) as comonomer in the miniemulsion process. Previous

* To whom correspondence should be addressed. E-mail: shangr@zju.edu.cn.

10.1021/ma052061t CCC: $33.50
Published on Web 03/07/2006

Table 1. Basic Recipe of the Miniemulsion Polymerization Process

	steam A			steam B				steam C
component	water	SDS	buffer	octane	MPS	styrene	HD	KPS
amount/g	150	0.2	0.3	8.33	1	3.33	0.6	0.3

research on latex stability and the control of hybrid microstructure[13] when using this functional monomer in hetrophase polymerization process make it possible to synthesis hybrid nanocapsules in one step by this process. At present, the effects of operating parameters on the formation of the latex morphology are analyzed in detail. All these parameters can be attributed to three aspects in the reaction process: particle nucleation mechanism, phase behavior in droplets, and thermodynamic and kinetic factors which determine the final morphology (interfacial tension of the particles and mobility of polymer in droplets).

Experimental Section

Materials. Styrene (from Aldrich) was distilled under vacuum before use. 3-Trimethoxysilylpropyl methacrylate (MPS, Aldrich) was used as comonomer without any purification. Octane was used as low molecular weight hydrocarbon nonsolvent for template. Potassium persulfate (KPS, Acros Organics) was used as initiator, sodium dodecyl sulfate (SDS) as surfactant, and hexadecane (HD) as costabilizer. Equivalent quantities of ammonium dihydrogen phosphate and disodium hydrogen phosphate were used as pH buffer to fix a neutral medium.

Synthesis of the Capsules. Unless noted otherwise, the recipe for the miniemulsion polymerization is listed in Table 1. Surfactant and pH buffer agents are dissolved in water (steam A), and then the octane solution of monomer and hexadecane (steam B) was added and mixed. After ultrasonic dispersion for 4 min, they are warmed to 70 °C and initiator (steam C) was added to start the polymerization. The initial charge and monomer feeds were protected with nitrogen during the polymerization. For about 180 min after reaction beginning, overall conversions achieve nearly 100% and then keep up the temperature at 70 °C for 1 h.

Characterization of the Capsules. TEM was performed with a JEOL JSM-1200EXT20 electron microscope operating at 80 kV. In a typical experiment, one drop of the colloidal dispersion was put on a carbon film supported by a copper grid and allowed to air-dry before observation. The diameter, D_p, of the latex particles was determined by dynamic light scattering (DLS) using a Malvern Zetasizer 3000HSA instrument. Infrared spectra were recorded using a Nicolet FTIR 560 spectrometer on powder-pressed KBr pellets. ^{29}Si solid-state NMR measurements were performed on a Bruker DSX-300 spectrometer operating at 59.6 MHz by use of cross-polarization from protons. The contact time was 5 ms, the recycle delay 1 s (sufficient for a full relaxation of protons), and the spinning rate 5 kHz. The ^{29}Si NMR spectra were simulated using the DM-FIT program for quantitative analysis. The samples were prepared by first centrifuge and then dried under vacuum at 50 °C for 5 h.

Characterization of the Loading and Release Process of the Capsules. Anthracene is dissolved in THF first; a certain amount of these nanocapsules is added into the solution. The diffusion processes of anthracene into the capsules are monitored by ultraviolet−visible measurement (the characteristic adsorption of anthracene is 367 nm). After equilibrium that the anthracene diffused into capsules, the mixture was centrifuged and washed to remove the supernatant anthracene. Parts of latex particles are dried for IR analysis, and the other parts of them are redispersed in THF and followed by UV measurements continuously to monitor the release process of anthracene.

Results and Discussion

Synthetic Process of the Capsules. The schematic supposed in Figure 1 can serve as a starting point to describe this process for making hybrid capsules in detail.

First, monomers (styrene and MPS) and costabilizer (HD) are dissolved in the hydrocarbon octane; then miniemulsion of the mixture was formed by a homogenization process (sonication) after the mixture was put into aqueous surfactant (SDS) solution. So the small droplets composed of monomers and hydrocarbon were formed, which is stabilized by the co-effect of SDS and HD. When water-soluble initiator (KPS) was added, it was thermally decomposed to generate primary free radicals in aqueous phase and then propagates to be oligo-radicals and entry into monomer droplets for polymerization. However, if not right formulation is chosen, micelles may exist in the system and generate particles; also, the radicals can continuously propagate in the aqueous phase and precipitate to generate solid spheres. Therefore, the particle nucleation method is of great importance to the final morphology of latex. Here, we first present a comparison of the morphology formed by two extreme particle nucleation methods with same recipe: droplet nucleation in miniemulsion polymerization process and micelle nucleation in conventional polymerization process (in conventional emulsion polymerization process, HD was not added), which was proved by particle growth results (see Supporting Information). Figure 2 is the morphology of the latex obtained by these two different polymerization processes. The conventional system leads in no case to the formation of capsules because octane cannot transport from the large droplets to the polymerization sites (particles), while miniemulsion system improves the perfection of polymer capsule morphology.

When particles dominantly generated by droplets after the operation condition are controlled, polymer is built in droplets. Octane is a nonsolvent for polystyrene and its copolymer, and as monomer is consumed, the polymer becomes progressively

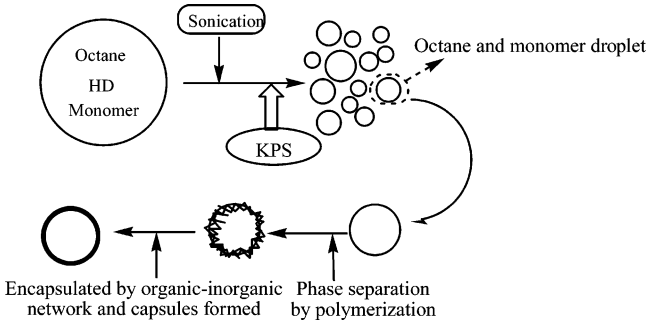

Figure 1. Schematic representation of the formation of the hollow capsules.

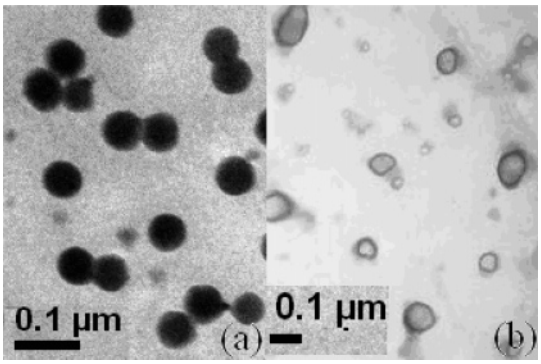

Figure 2. TEM images of the latex synthesized by (a) conventional emulsion polymerization and (b) miniemulsion polymerization.

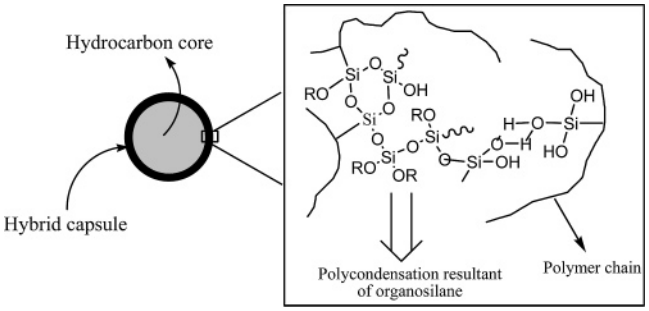

Figure 3. Schematic representation of microstructure in the hybrid capsule.

Table 2. Latex Particle Diameters Measured by TEM and DLS and the Void Fraction

diam of latex particles/nm		void fraction/%	
determined by TEM	97	calculated by TEM result	9758.3
determined by DLS	101.5	calculated by feed recipe	61.0

less compatible with the dispersed hydrocarbon/monomer mixture. Phase separation of polymer is observed to occur primarily at the interface of the particle (see Supporting Information). This phase behavior in droplets also has great influence on the final morphology: if the produced polymer cannot separate out immediately, this will result in a monomer-rich hydrocarbon phase, which can solubilize the polymer. This leads to single-phase polymer particles, and the phase behavior in the droplets is again dependent on the formulation of the polymerization process.

After polymer was separated out, the final morphology in polymer microparticles involves the thermodynamic factor which had been analyzed by Sundberg et al.[14] and a kinetic factor which mainly includes the polymerization locus and viscosity during the polymer diffusion process. In this case, the copolymer−water interface is believed to have the lowest interfacial energy in system (this will be calculated in the following part). In addition, the water-soluble thermal initiator generates radicals, including oligo-radicals, which are adsorbed and anchored to the surface of the dispersion, so the surface appears to become the primary site for polymerization. Both lead to polymer encapsulate the hydrocarbon at the surface of the particles and to form capsules.

For the evolution of microstructure along with copolymerization reaction, the organosilane in MPS was easily hydrolyzed into silanetriols when contacted with water, and the silanetriols were metastable and self-condensed to yield the hybrid microstructure shown in Figure 3, which are characterized by our previous work.[13]

Characterization of the Morphology and Microstructure of the Nanocapsule. The TEM images of the nanocapsules are shown in Figure 2b. It is clearly revealed the hollow structure of the latex. The average particle size of the latex measured both by TEM and DLS is about 100 nm. The void volume is also characterized by TEM, and it is consisted with predicted value calculated by the feed recipe very well (it is assumed all of octane is encapsulated by polymer in the calculation) (see Table 2). It indicates that most of octane is encapsulated by polymer to form capsules.

Figure 4 shows the IR spectra of the latex obtained at the end of the reaction. We note the absence of the C═C bond of MPS at 1630 cm^{-1} which indicates complete conversion of (co)-monomers by free radical (co)polymerization. We also observe in Figure 4 a signal at 821 cm^{-1} characteristic of nonreacted SiOR groups (νSi−O−C) decreases a lot, indicating the hydrolysis of SiOR groups.

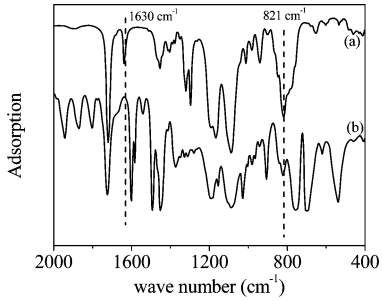

Figure 4. FTIR spectra of (a) pure MPS and (b) hybrid capsules.

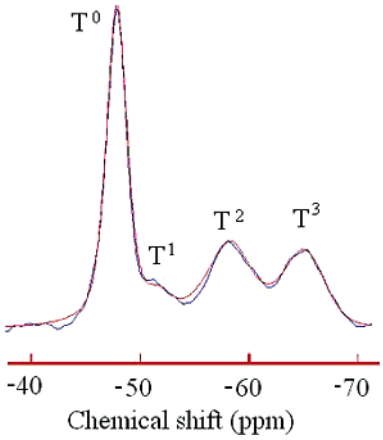

Figure 5. ^{29}Si solid-state NMR spectra of the hybrid capsules.

In the ^{29}Si solid-state NMR spectra (see Figure 5) of the latex particles, it is found parts of T^0 are condensed to T^2 and T^3 (the different silicon-based species are named according to the conventional T^j nomenclature where T is the trifunctional alkoxysilane and j designates the number of siloxane groups bounded to the silicon atom), which confirms the formation of the microstructure described in Figure 3. The condensation degree of the products is about 39.3%, which is calculated by DOC (degree of condensation) = $(T^1\% + 2T^2\% + 3T^3\%)/3$. To summarize, the copolymer chain is the main structure in the hybrid shell; however, a large number of SiOR groups are hydrolyzed and condensed to form Si−O−Si network, which contributed to the hybrid structure.

Thermodynamic and Kinetic Aspects to the Final Latex Morphology. (a) Thermodynamic Equilibrium. In dealing with the thermodynamics of encapsulation in an emulsion polymerization, there has been a significant development of ideas in the literature. Thermodynamic control of the particle morphology has been described predominantly in terms of the interfacial energies between the components. Sundberg et al.[14] presented a thermodynamic model to determine the morphology thermodynamically favored. They suggested that each particular morphological configuration has a different Gibbs free energy, which can be obtained by $G = \sum(\gamma_i A_i)/\sum A_i$ (A_i is the area of each interface). The arrangement with the minimal free energy will be the one that is thermodynamically favored.

In this case, there are four possible morphologies: capsules, polymer in center, individual particles and droplets, hemispheres of polymer and octane. The interfacial tension of each interface is listed in Table 3 (the surface tension of copolymer is calculated by linear summation according to volume fraction of pure polymer).

The Gibbs free energy with different morphology calculated is shown in Table 4. It is well revealed that the morphology of capsules leads to the lowest interfacial tension, so polymer is

Table 3. Surface and Interfacial Tension of Different Phase

		water	octane	PS	poly(MPS)	PS-*co*-MPS
surface or interfacial tension/mNm^{-1}	air	72.8[15]	23.5[15]	40.7[16]	44.8[16]	41.6
	water		50.8	22.0	14.4	21.1
	octane			7.2	10.4	7.6

Table 4. Free Energy of the Latex with Different Possible Morphology

	free energy of the latex per area (mN m^{-1})			
MPS fraction in polymer	capsules	polymer in center	individual particles	hemispheres
pure PS	15.7	36.5	42.0	26.7
[MPS] = 22.5 wt %	14.6	37.5	38.9	25.2

inclined to localize on the surface of droplets. The existence of MPS units in the copolymer makes the Gibbs free energy of capsule morphology even less because of the relatively hydrophilic groups like SiOR groups (see Table 4), which increase the driving force to the formation of capsule morphology. Furthermore, Si−OR groups can be hydrolyzed and condensed to much more hydrophilic groups like SiOH groups, which decrease the surface tension of the shell even more (the real Gibbs free energy of the hybrid capsules must be much slower than what is shown in Table 4) due to their strong attraction with the aqueous phase.

(b) Kinetic Analysis. The most favorable morphology determined by thermodynamic analysis may not be formed finally because of the resistance to flow. It arises form viscous drag when the final morphology makes it necessary that the resulted polymer must migrate from the locus they produced. In our case, the surface of droplets becomes the locus of polymerization of phase separation, and the monomers are supplied from the droplets inside because anionic radicals and oligo-radicals formed in the aqueous phase are kept on the surface of droplets when they diffused into the latex due to the anionic surfactant. Therefore, the resulting polymer needs not the migration process to encapsulate hydrocarbon, which is in favor of the formation of capsule.

Variables. (a) Influence of Surfactant Amount. In general, the miniemulsion is composed of submicron monomer droplets stabilized with a surfactant against coalescence and with a costabilizer to minimize Ostwald ripening. The fraction of particles generated by droplet nucleation depends on the number of droplets and micelles and on the relative values of the rate coefficients for entry of radicals into monomer droplets and micelles and the propagation rate in the aqueous phase. The presence of micelles depends on the amount of surfactant and the homogenization procedure.

In our case, a high enough intensity (sonication under 600 W) in the homogenization procedure is used with enough time to minimize the presence of micelles by this reason. So the surfactant amount is the main reason to produce micelles, and whether micelles are existed in the system is proved by surface tension measurement (see Supporting Information). Here, two surfactant amounts are compared, and the surfactant concentrations in aqueous phase are 3.3 and 1.3 g/L, respectively, which represent the existence of micelles or not. The evolution of particle size and number-average particle size distribution as a function of conversion was shown in Figure 6. When surfactant concentration is 1.3 g/L, the particle size distribution keeps the same shape and particle size only increased slightly. This is indicative of nucleation occurring primarily in the miniemulsion droplets. Meanwhile, in the system the surfactant concentration is 3.3 g/L; new particles are generated continuously and become the dominant part relative to the particles generated in the initial phase (see Figure 6b).

Therefore, the morphology determined by TEM images (see Figure 2b and Figure 7) is quite different in these two cases. The predominately droplet nucleation leads to the perfection of polymer capsule morphology, while the particles present quite different morphology. This also proved the complicated nucleation mechanisms as indicated by the evolution of particle size and its distribution. In addition, it is has been reported that, with an increase in the concentration of surfactant, the coverage of the surfactant on the particles increases quickly,[10] which significantly reduces the interfacial tension between water/particle. Therefore, it is reasonable to assume that the difference in the water/polymer and water/hydrocarbon interfacial tension

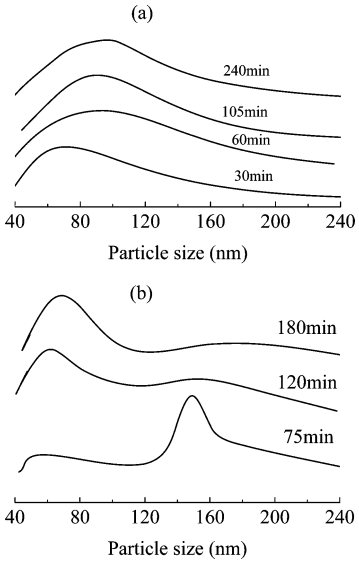

Figure 6. Evolution of particles size distribution (volume average) as a function of time: (a) surfactant concentration is 1.3 g/L; (b) surfactant concentration is 3.3 g/L.

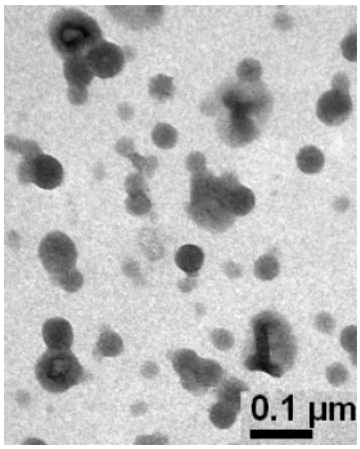

Figure 7. TEM images of latex with high surfactant concentration.

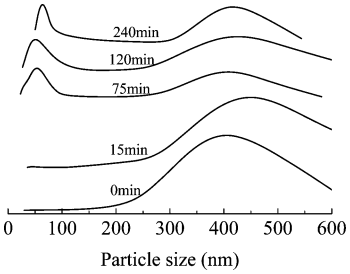

Figure 8. Evolution of particles size distribution (volume average) as a function of time when costabilizer is cetyl alcohol.

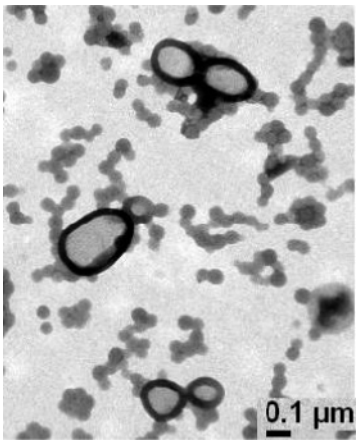

Figure 9. TEM images of latex with cetyl alcohol as costabilizer.

is narrowed at high surfactant concentration and harms the encapsulation.

(b) Influence of Costabilizer Type. From the study above, micelles can be avoided by adjusting the surfactant concentration. Under this circumstance, the fraction of the polymer particles generated by droplet nucleation is determined by the fraction of radicals captured by the monomer droplets relative to the fraction that precipitates in aqueous phase producing particles by homogeneous nucleation. The fraction of radicals captured by the droplets depends on the number of droplets and on the rate of radical entry.

For miniemulsions containing cetyl alcohol, early work[17,18] showed that homogeneous nucleation was difficult to avoid. This process presented a relative slow nucleation stage, and both of these were attributed to a reduced radical adsorption rate. In Figure 8, the particle size distribution with double peak is well revealed in the simultaneous two particle nucleation methods. Large particles about 400 nm existed from the beginning of the polymerization; the particle size and its distribution did not change much, which indicated that they are generated by droplet. Along with the polymerization, new particles with small particle size are generated by homogeneous nucleation. As shown in Figure 9, the small particles generated by homogeneous nucleation are solid while still some larger particles with capsule morphology are believed to be generated by droplet nucleation.

(c) Influence of Monomer/Octane Ratio. Polymer is produced in droplets when the polymerization reaction starts. The instantaneous composition (especially in the initial phase of polymerization) in the droplets is critical to producing the desired morphology. The immediate phase separation is needed when polymer is produced, which requires the mixture of monomer and octane to be a nonsolvent for polymer. If the droplets cannot become two phase immediately as polymer produced, it will results in a polymer-rich hydrocarbon phase

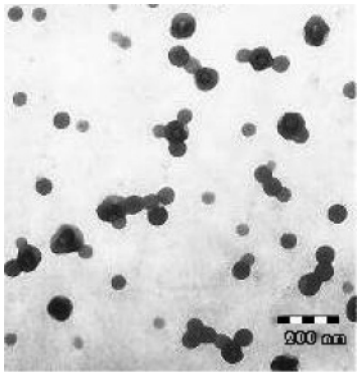

Figure 10. TEM images of latex with monomer/octane ratio of 1:1.

with quite high viscosity. Even in the later phase, polymer is inclined to separate out according to thermodynamic criteria; the polymer in droplets is hard to be separated because the high viscosity prevents the movement of polymer chain. The droplets are the mixture of octane and monomer, and octane is a nonsolvent for polymer while monomers are good solvent for polymer. Therefore, the monomer/octane ratio is a key parameter, and it is best to keep the homogeneous phase on the verge of becoming two phases (polymer cannot be dissolved in the mixture of droplets).

It can be estimated by the $\sigma_v-\sigma_h$ graph whether the mixture in droplets can dissolve the polymer, and the $\sigma_v-\sigma_h$ graph is believed to the most effective method to predict the solubility of polymer in solvents.[19] The results predicted by solubility parameters (see Supporting Information) showed that only when the monomer/octane ratio is less than 1:1.94 can polymer be separated out immediately as it was produced. This result is also proved by experiments (see Supporting Information). It is also revealed that when the monomer/octane ratio is increased, the polymer solubility is increased correspondingly. When this ratio is larger than approximately 1:2, the solubility increased suddenly. Therefore, a relatively small monomer/octane ratio (1:1.86) is chosen in the recipe in order to obtain the desired morphology as shown in Figure 6. An example carried out by higher monomer/octane ratio (1:1) is compared. From the TEM images (see Figure 10), it is found that no hollow morphology is obtained in this example as we have analyzed.

(d) Influence of MPS Fraction in Monomer. When MPS is introduced into the polymer chain the surface tension decreased, which is in favor of the formation of capsules as we analyzed above. The more MPS is introduced into the polymer, the more the surface tension decreased. For this point of view, MPS help polymer encapsulate hydrocarbon. However, as the results we obtained before,[13] the T_g of hybrid products decreased with increased MPS concentration because the copolymer contained more and more siloxane units resulting from hydrolysis−condensation reactions, which is very flexible. This decreased the mechanical properties of the capsules and made the capsules easy to collapse as shown in Figure 11.

Loading and Release Process of the Capsules. Many applications of capsules are based on the permeability of the capsule wall. For example, polymer nanocapsules have been proved that they are potential drug carrier for controlled delivery. Furthermore, it is possible to enable the delivery of large species such as protein and genes. In the present paper, anthracene is used as a model compound in an organic solvent for the initial investigation.

The loading process was described first. According to Fick's law, when labels diffused into the capsules, the label concentra-

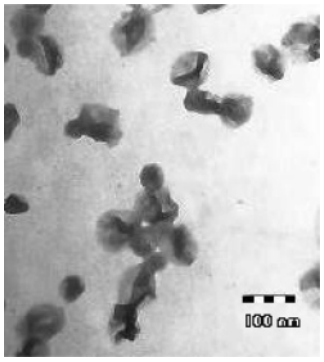

Figure 11. TEM images of latex with [MPS] = 50 wt % in the hybrid shell.

tion out of the capsules c_w can be expressed as followed:

$$dc_w/dt = -A(c_w - c_v) \quad (1)$$

where c_v is the label concentration inside the capsules. It can be integrated as

$$c_w = c_0 e^{-At} \quad (2)$$

where c_0 is the initial label concentration and

$$A = PS/V = 3P/r = 3D_B/rh \quad (3)$$

D_B is the effective diffusion coefficient; r and h are the radius and the thickness of the capsules, respectively.

As described by the previous model for the permeation process,[20] the UV adsorption intensity can be expressed as follows:

$$I(t) = \varphi_w n_w + \varphi_v n_v \quad (4)$$

where φ_w and φ_v are the UV quantum yields in the bulk and the capsule cavities, respectively; n_w and n_v are the number of the label molecules in the bulk and the capsule cavities, respectively. From eq 2

$$n_w = n_0 e^{-At} \quad (5)$$

substituted into eq 4

$$I(t) = n_0\varphi_v + (\varphi_w - \varphi_v)e^{-At} \quad (6)$$

because

$$I(t{=}\infty) = n_0\varphi_v \quad \text{and} \quad I(t{=}0) = n_0\varphi_w \quad (7)$$

thus

$$I = [I(t) - I(t{=}\infty)]/[I(t{=}0) - I(t{=}\infty)] = e^{-At} = e^{-3D_B t/rh} \quad (8)$$

The loading kinetic curve is shown in Figure 12, and the solid lines are the curves simulated by eq 8; it is observed that the experimental data are fitted with the calculated results quite well. The efficient diffusion coefficients calculated by the model is 1.84×10^{-15} cm^2 s^{-1}.The FTIR spectra of anthracene (a), pure nanocapsules (b), and the capsules after loading of anthracene (c) are shown in Figure 13. It is found that the adsorption of anthracene at 725, 883, 955 cm^{-1} appeared in the spectrum of the nanocapsules after loading of anthracene, which proved the anthracene is loaded into the capsules.

The kinetic curve of the releasing process is shown in Figure 14. It is revealed that the diffusion rate of the releasing process

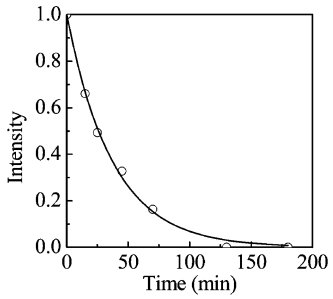

Figure 12. Diffusion kinetics of the anthracene loading process (—, calculated by model).

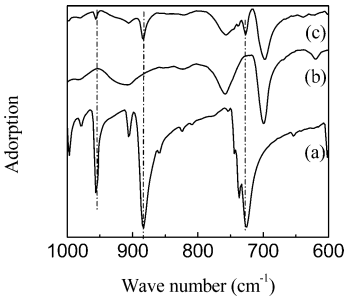

Figure 13. IR spectra of anthracene (a), capsules (b), and anthracene loaded capsules (c).

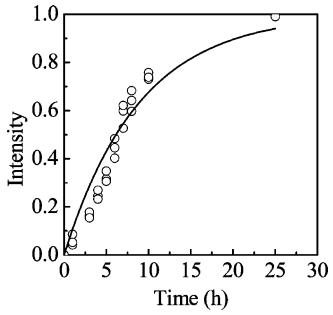

Figure 14. Diffusion kinetics of the anthracene releasing process (—, calculated by model).

is much lower than the loading process. Using a similar method with the loading process, the relation between the adsorption intense of UV and time can be expressed as follows:

$$I = [I(t) - I(t{=}0)]/[I(t{=}\infty) - I(t{=}0)] = 1 - e^{-3D_e t/rh} \quad (9)$$

The effective diffusion coefficient of the releasing process is about 8.24×10^{-17} cm^2 s^{-1}, which is much lower than that of the loading process. This is due to the microstructure of the capsules. The SiOR groups in MPS units can be hydrolyzed and condensed to much more hydrophilic groups like SiOH and Si−O−Si groups, so that these groups are inclined to exist on the outside of the capsules and styrene units can more easily stay inside. Therefore, the label molecule (which is quite hydrophobic) is much more difficult to diffuse out through the pores in the capsule's wall because of the hydrophobic repulsive effect.

Conclusion

Organic−inorganic hybrid nanocapsules were synthesized in one step: styrene and functional comonomer MPS were copolymerized in miniemulsion droplets to form capsule morphology. Along with the copolymerization process, hydrolysis and polycondensation have taken place, resulting in cross-linking of the alkoxysilane monomer.

The nucleation method is of great importance to the final morphology. Dominant droplet nucleation made the perfection of polymer capsules morphology while micelle and homoge-

neous nucleation will lead to solid particles. Low surfactant concentration in the formulation is necessary to avoid the existence of micelle nucleation, and the costabilizer cetyl alcohol is not recommended because it promoted homogeneous nucleation.

When polymer was built, it must be separated out immediately in droplets, or it will result in polymer-rich single-phase particles. To make the built polymer separate immediately, the monomer/octane ratio must be less than 1:2, and more MPS fraction in monomer will favor in producing capsules but decrease the mechanical properties.

This kind of nanocapsule can be used in loading and releasing active substances. For example, the efficient diffusion coefficients in loading and releasing process of anthracene are 1.84×10^{-15} and 8.24×10^{-17} $cm^2\ s^{-1}$, respectively.

Acknowledgment. The authors are indebted to the New Century Excellent Scholar Supporting Program of Chinese Education Ministry for financially supporting this work.

Supporting Information Available: Evolution of particle size as a function of conversion by conventional emulsion polymerization and miniemulsion polymerization; phase separation observed by TEM images along with the polymerization; surface tension measurement at different SDS addition amount; soluble parameters of different parts in the mixture droplets; polymer solubility at different monomer fraction in the mixture droplets. This material is available free of charge via the Internet at http://pubs.acs.org.

References and Notes

(1) Tissot, I.; Novat, C.; Lefebvre, F.; Bourgeat-lami, E. *Macromolecules* **2001**, *34*, 5737.
(2) Imhof, A. *Langmuir* **2001**, *17*, 3579.
(3) Mandal, T. K.; Fleming, M. S.; Walt, D. R. *Chem. Mater.* **2000**, *12*, 3481.
(4) Blomberg, S.; Ostberg, S.; Harth, E.; Bosman, A. W.; Van Horn, B. *J. Polym. Sci., Part A* **2002**, *40*, 1309.
(5) Huang, H.; Remsen, E. E.; Kowalewske, T.; Wooley, K. L. *J. Am. Chem. Soc.* **1999**, *121*, 3805.
(6) Zhang, Q.; Remsen, E.; Wooley, K. L. *J. Am. Chem. Soc.* **2000**, *121*, 3642.
(7) Liu, X.; Jiang, M.; Yang, S.; Chen, M.; Chen, D.; Yang, C.; Wu, G. *Angew. Chem., Int. Ed.* **2002**, *41*, 2950.
(8) Pavlyucheko, V. N.; Sorochinskaya, O. V.; Ivanchev, S. S.; Klubin, V. V.; Kreichman, G. S.; Budtov, V. P.; Skrifvars, M.; Halme, E.; Koskinen, J. *J. Polym. Sci., Part A* **2001**, *39*, 1435.
(9) Mcdonald, C. J.; Bonck, K. J.; Chaput, A. B.; Steven, C. J. *Macromolecules* **2000**, *33*, 1593.
(10) Tiarks, F.; Landfester, K.; Antonietti, M. *Langmuir* **2001**, *17*, 908.
(11) Brandriss, S.; Margel, S. *Langmuir* **1993**, *9*, 1232.
(12) Bourgeat-Lami, E.; Tissot, I.; Lefebvre, F. *Macromolecules* **2002**, *35*, 6185.
(13) Ni, K. F.; Shan, G. R.; Weng, Z. X; Sheibat-Othman, N.; Fevotte, G.; Lefebvre, F.; Bourgeat-Lami, E. *Macromolecules* **2005**, *38*, 7321.
(14) Winzor, C. L.; Sundberg, D. C. *Polymer* **1992**, *33*, 3797.
(15) Dean, J. A. *Lange's Handbook of Chemistry*, 13th ed.; McGraw-Hill Book Co.: New York, 1972; pp 10.98−10.116.
(16) Brandrup, J.; Grulke, E. A.; Eric, A.; Immergut, E. *Polymer Handbook*; Wiley-Interscience: New York, 1999; Vol. VI, pp 521−541; Vol. VII, pp 675−714.
(17) Hansen, F. K.; Ugelstad, J. *J. Polym. Sci., Polym. Chem. Ed.* **1979**, *17*, 3069.
(18) Choi, Y. T.; El-Aasser, M. S.; Sudol, E. D. *J. Polym. Sci., Polym. Chem. Ed.* **1985**, *23*, 2973.
(19) Van Krevelen, D. W. *Properties of Polymers: Their Estimation and Correlation with Chemical Structure*; Elsevier Scientific Publishing Co.: Amsterdam, 1976.
(20) Ding, J.; Liu, G. *J. Phys. Chem. B* **1998**, *102*, 6107.

MA052061T